OCEAN TIDE LOADING AND DIURNAL TIDAL MOTION OF THE SOLID EARTH CENTRE

Hans-Georg Scherneck, Chalmers University of Technology
Frank H. Webb, Jet Propulsion Laboratory

INTRODUCTION

Ocean tides imply mass movements on a global scale and whence the relative locations of the mass centre of the solid earth and that of the ocean are subject to temporal variations. Assuming that only the solid earth (and unless expressly noted otherwhise: jointly the core) counterbalance the oceanic mass dislocation in order to maintain a uniformly moving centre of gravity of the entire planet, the offset of the solid earth mass centre from the joint mass centre due to ocean tides can be readily computed.

The conventional models for ocean loading displacements (McCarthy, 1996; Scherneck, 1991) do not include the motion of the frame origin; they specify only the displacements due to deformation and that these displacements are reckoned with respect to the centre of gravity of the solid earth. Note,however, that this concerns all spherical harmonic degrees including 1, which is an excentric mode.

The formulation of tidal motion in terms of a finite number of partial tides, each having a specific frequency, allows that at any location on the earth suface the loading tide displacement can be computed from a finite set of amplitude and phase parameters. The parameters vary significantly from place to place, reflecting an integrating property of the loading effect due to masses within some hundred kilometers radius around the observing point. The convention for the phase is to have zero phase of the astronomical tide gravity potential at the zero meridian. The same harmonic setup is suitable also for the centre of gravity movements of the solid earth.

The number of amplitude and phase parameters can be much lower than the number of tidal harmonics usually included in harmonic developments of the tide potential. The complex coefficient combining phase and amplitude of the effect can be interpolated as a function of frequency within each tide band, using a low order polynomial. A special interpolation method using sinusoids instead of polynomials is found in the orthotide formulation (Groves and Reynolds, 1975). The orthotide approach has been employed by the CSR group (Eanes and Bettadpur, 1995). In the interpolation the tidal spectrum must be stripped of waves pertaining to spherical harmonic degrees greater than two since the ocean response to these forcings is fundamentally different. At present, ocean tides excited by degree three tides and above are not included in the loading model. On the planetary scale we expect them to be 1/60 smaller than the degree two tides, and thus we dismiss them from the geocentre case.

The stations operating for the maintenance of geodetic reference systems are attached to the solid earth. According to our reasoning about the mass centre of the solid earth we submit that after reduction of the deformation component of loading tides the global network is seen to undergo small oscillations around the physical mass centre. It is this motion that will be termed—a bit misleadingly perhaps—geocentre tide.

The geocentre tide has the simple nature of a rigid translation. As a consequence, observing techniques that are based on simultaneous differences of positions or ranges like VLBI are inherently invariant to it.

To predict the tidal motion with respect to the joint mass centre it is practical to combine the two contributions. Interpolation of admittance can be applied before or after combination. The deformation can be added to the local solid earth tide as the latter is inherently free from global translation.

1 Until now ocean loading tide model did not include geocentre tide

The IERS recommended ocean loading tide model did not include the geocentre tide for the following reasons:

Whereas the deformation part obtained from different ocean tide maps is within relatively small bounds, the geocentre terms show considerable spread. Table 1 shows representatively the geocentre tide coefficients for the M_2 and O_1 tides. Hydrodynamic models of the ocean are relatively inaccurate as regards long-wavelength features since the dynamic terms are related to the gradient of the surface elevation. In this sense degree one efficient terms in the ocean are at the extreme low-admittance end of the signal that is passed through the gradient operator. In lieu of observational verification of degree-one oceanic tides or conversely the geocentre tides their inclusion in a reference standard would be premature.

As a second reason, the reference point for satellite orbits must be chosen consistently with the local site motion of the tracking stations. If the geocentre tide were applied at observing stations without the orbit referring to the joint mass centre, a geocentre tide with the negative sign would be introduced into the reduced observations. Thus, there is a risk of inconsistent application of the geocentre tide.

In the near future, however, a higher level of consistency can be reached. The CSR3.0 ocean tide model appears to be suitable for a number of effects (geopotential, geocentre, ocean loading). The long-period tides can in this context be treated as a static equilibrium response, which is the assumption of CSR3.0. The fortnightly ocean tide might show significant departures from a static response; due to ongoing efforts of the Le Provost group (Lyard, 1998, pers. comm.) a dynamic M_f model is available since May 1998.

2 Estimating ocean loading tides from GPS

Single point positioning results can be obtained from GPS with GIPSY software (Webb and Zumberge, 1993; Zumberge et al., 1997). We have chosen this processing mode since it does not perform range differencing, and since it is free from the interdependencies of motions and errors at simultatneous observations typically experienced in network solutions. Thus the data is expected to preserve a more complete set of range variations between the satellite and the receiver. Spacecraft positions are taken from JPL orbit solutions which include an accurate clock parameter as a prerequisite to solve single point positions accurately. The huge amount of available observations allows to solve for long, almost uninterrupted time-series at sampling rates suitable for tide analysis.

Positions were estimated with the GIPSY Kalman filter at two hours interval, atmospheric parameter at

Table 1: Coefficients for geocentre tides, cos and sin factors, repectively for motion along the three cartesion components Z, X and Y. Unit is millimetre. The data are based on ocean tides due to L - Le Provost et al. (1994), C - CSR3.0 (Eanes and Bettadpur, 1995), S - Schwiderski and Szeto (1981). Model CW lists the geocentre results of Watkins and Eanes (1997).

Tide	Model	Z		X		Y	
		cos	sin	cos	sin	cos	sin
M2	S	-0.60	-0.84	-4.29	-0.68	2.98	-1.71
M2	L	-1.68	-2.23	-0.49	-0.67	0.04	-0.77
M2	C	-1.44	-1.53	-1.46	1.30	1.34	0.05
M2	CW	-2.72	-1.50	-2.38	0.34	1.67	0.62
O1	S	-0.52	2.47	-1.00	-0.03	-1.02	-1.09
O1	L	-1.04	3.87	-0.88	-0.61	-0.93	-0.99
O1	C	-0.40	2.93	-1.11	-0.19	-0.97	-0.85
O1	CW	-0.46	3.27	-2.85	-0.64	-1.65	0.45

5 minutes interval assuming a random walk noise model of the zenith delay. Each sample was taken to represent the mean position of the station at the central time of the two-hour interval. The 3-D series were transformed into a local system with east, north, and vertical axes. Solid earth tide displacements were subtracted as usual in GIPSY.

Each component of the position time series was analyzed for remaining tides by least-squares estimates of complex admittance parameters for tidal wavegroups which are constructed from the tide potential of Tamura (1987). Admittance parameters for a linear trend and for a time series of predicted atmospheric loading displacements were also included in the analysis.

Computation of atmospheric loading followed closely the method for ocean loading tides, the major difference being that loading occurs on land, and that the inverse barometer assumption suggested us to exclude waters with a depth greater than 300 m from being loaded. As a side-effect of the data preparation, geocentre tides computed from atmospheric pressure were made available to the community (cf Appendix). They are based on ECMWF ground-level fields at six hours interval.

The results are compared to ocean loading parameters computed along the lines of Scherneck (1991) and IERS Conventions (McCarthy, 1996) with the following modifications:

- Loading deformations (i.e. excluding geocentre tide) due to ocean tide models of Schwiderski and Szeto (1981) (shorthand: S), Le Provost et al. (1994) (L), and CSR3.0 (Eanes and Bettadpur, 1995) (C);
- Adding the geocentre tide as derived from each of these models to the deformation (SG, LG, CG).
- Adding a degree one co-oscillating ocean tide to the wet nodes of CSR3.0 in order to obtain a geocentre tide compatible with recent SLR observations (Watkins and Eanes, 1997) and computing loading deformation and geocentre tide (CWG).

The CSR3.0 model was always masked with the land-sea distribution of the L model as it specifies many wet nodes at obvious land locations.

2 Discussion

The least-squares analysis results show clearly that ocean loading tides can be resolved in GPS data at the 1 mm level. Observed lunar species correlate well with the models in all three spatial components. Few authors have looked at the horizontal components before. In the light of the small error ellipses the data appears powerful and promising. Exploring the relation between the formally derived sigma and the post-fit residual χ^2, the sigma shown on the horizontal components is a cautious estimate by a factor of typically 1.5. For more explicit results we refer to the sideshow, see Appendix.

We show three typical cases in the form of phasor graphics, Reykjavik, Iceland (M_2) - figure 1; Irkoutsk, Siberia (M_2) - figure 2; and Mauna Kea, Hawaii (O_1) - figure 3. Solar tide oservations are not further interpreted since re-initialisation of the Kalman filter occurred at a 24 hour interval. We also hesitate to interpret sidereal tides as large effects at K_1 and its upper harmonics are found. They might be related to orbit errors, features that change only slowly in time when watched in a nonrotating frame). Thus, the leading partial tides that can be studied with prospective confidence are lunar species, M_2, N_2, O_1, and Q_1. The long duration of the time series warrants the required spectral resolution of the major sideral, solar, and in particular the lunar waves.

The general picture emerging from the GPS analysis is that

1. any of the submodels explains the observed motion equally well; reduction of the observed signal RMS is regularly better than 50 percent.

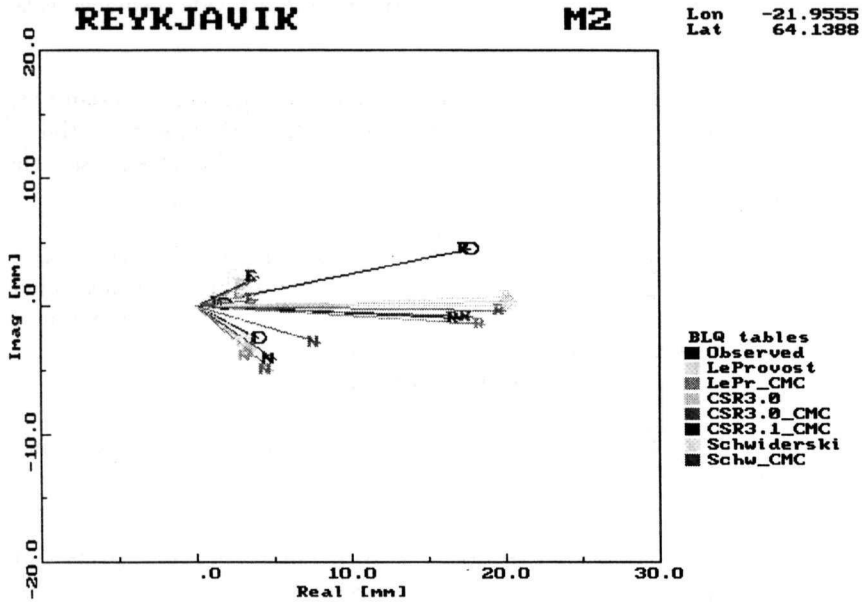

Figure 1: Phasor plot of tide analysis results. Solid earth tide has been reduced from the observations. The observations are shown in black with an error ellipse according to the a priori variance. Ocean loading tide models have been grey-coded with dark greys for models that include the geocentre tide and light greys for those that do not. From the post-fit error we find that the ellipse can be scaled up by 1.5 in the case of vertical displacement and down by 0.75 in the case of the horizontal components to achieve $\chi^2_\nu = \nu$.

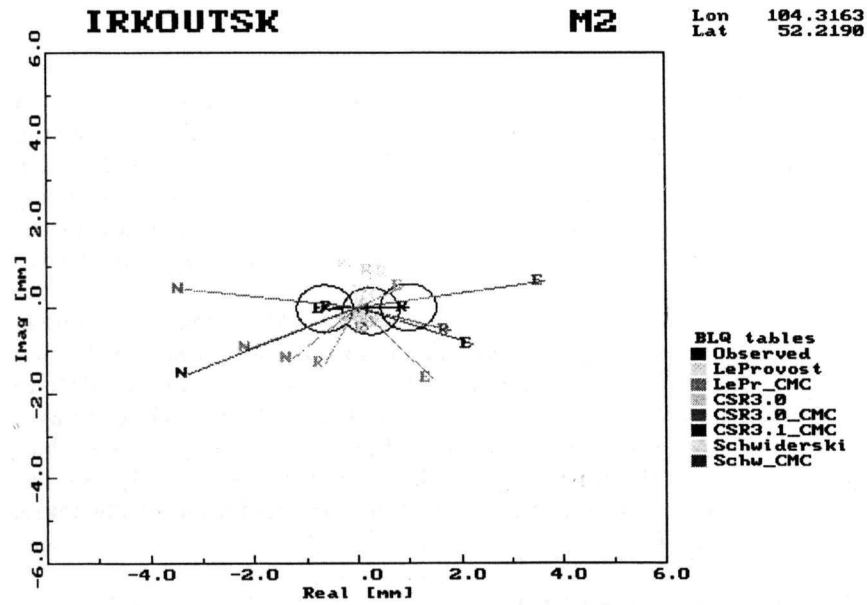

Figure 2: Far inland station Irkoutsk exhibits relatively strong geocenter motion as this global translation affects all locations equally much while ocean loading is rather small. Other caption information cf 1.

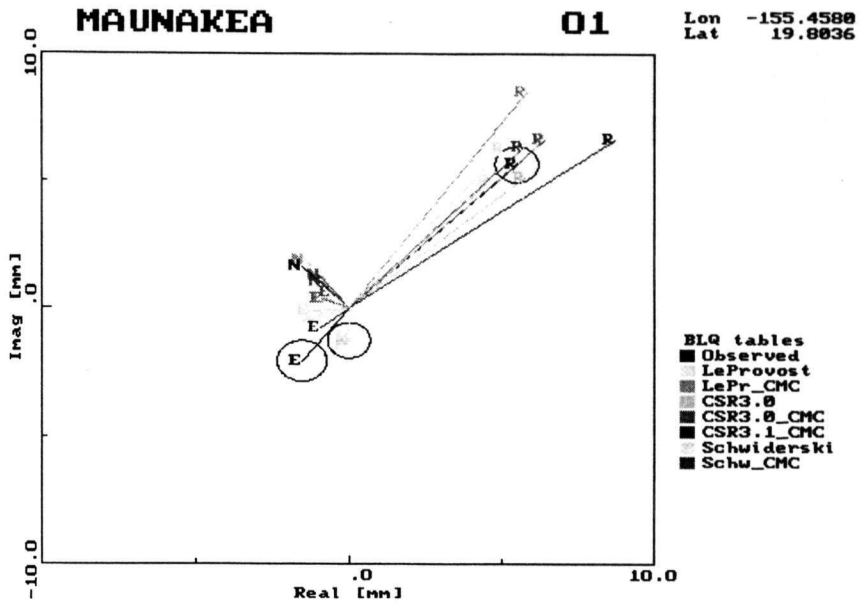

Figure 3: Diurnal residual tide O_1 at Mauna Kea, Hawaii. More caption information cf 1.

2. there are large residuals in terms of the formal confidence limits. Whether these residuals are due to systematic errors in the data analysis process or due to mismodelling remains to be determined.

3. most importantly, however, residuals increase when geocentre tides are included. This is most probably relating to the fact that geocentre tides were ignored in the process of computing the orbits. The computed orbits appear to be rather invariant to—at least short- period—rigid translations.

A superficial measure of the over-all impact of the loading options is the sum of squares of the tidal residuals at each station. The zero option, no ocean loading motion, is included. The sum

$$\begin{aligned} S_k^2 &= \sum_{n=1}^{N}\sum_{c=1}^{3} |u_{nc} - \hat{u}_{knc}|^2 \\ k &= \text{nil, S, SG, L, LG, C, CG, CWG} \end{aligned} \tag{1}$$

streches over the three spatical components and $N = 4$ lunar species as detailed above. The sums are presented in Table 2.

CONCLUSIONS

It is highly a matter of decisions to be taken at the satellite orbit computation centres whether or not to correct ranges observed at tracking stations for geocentre tides. For those developers who plan to employ the ocean loading model during the coming years there may be a desire for parallel options. End users need to carry out their procedures consistent with the orbit products etc. they acquire. In order to serve these demands and to accomplish a higher degree of consistency, the following suggestions will be made as regards the recommended IERS procedures:

1. Ocean loading models will come in two versions, with and without the geocentre terms. See Appendix.

2. The deformation as well as the geocentre tide will be computed with the CSR3.0 ocean tide as the basis.

Table 2: Root sum squares of lunar tides as observed with GPS, reduced by the ocean loading models based on ocean tides due to L - Le Provost et al. (1994), C - CSR3.0 (Eanes and Bettadpur, 1995), S - Schwiderski and Szeto (1981); modifier G designates inclusion of geocentre tide, CWG is CG modified to yield the geocentre motion of Watkins and Eanes (1997). Values are millimetres, σ designates error in determination of a single tide wavegroup.

Site	σ	nil	L	LG	C	CG	CWG	S	SG
Reykjavik	0.5	19.6	5.5	7.8	6.0	7.6	11.5	6.1	7.9
Sundsvall	0.5	3.7	2.8	5.3	2.8	4.9	9.5	3.2	6.4
Pie Town	0.5	5.6	1.9	5.3	2.0	4.9	9.0	2.4	6.1
HartRAO	0.8	16.4	12.5	13.2	11.8	10.8	12.7	12.6	13.4
Irkoutsk	0.5	2.1	2.7	5.8	2.8	5.4	10.0	2.7	6.9
Ascension	0.6	13.0	13.5	14.1	12.9	12.4	15.0	11.7	9.2
Yaragadee	0.5	7.5	14.6	16.3	13.8	15.0	16.8	13.9	15.2
Mauna Kea	1.1	14.5	3.6	7.2	6.1	8.7	12.3	4.0	7.4
Mendeleevo	0.5	2.6	1.7	5.5	2.0	5.0	9.4	2.0	6.5
Onsala	0.9	14.1	12.6	14.1	12.6	12.9	16.1	12.4	15.0

3. The recommended model in connection with GPS and VLBI will be the geocentre-free model OL-C, unless orbit computation centres make the transition to orbits centred on a tide-free origin.

4. The recommended model in connection with satellite methods that use a tide-free frame origin will be OL-CG.

5. The other models will be earmarked as being for experimental purposes.

REFERENCES

Eanes R.J. and Bettadpur S., 1995: The CSR 3.0 global ocean tide model, *Technical Memorandum CSR-TM-95-06,* Center for Space Research, University of Texas, Austin, Tx.

Groves, G.W. and Reynolds, R.W., 1975: An orthogonalized convolution method of tide prediction. *J. Geophys. Res.,* **80,** 4131–4138.

Le Provost, C., Genco, M. L., Lyard, F., Vincent, P., and Canceil, P., 1994: Spectroscopy of the world ocean tides from a finite element hydrological model, *J. Geophys. Res.*, **99**, 24777–24798.

McCarthy D.D. (ed.), 1996: IERS Conventions (1996), *IERS Technical Note 21,* July 1996, Observatoire de Paris.

Scherneck H.-G., 1991: A Parameterized Solid Earth Tide Model and Ocean Tide Loading Effects for Global Geodetic Baseline Measurements, *Geophys. J. Int.*, **106**, 677–694.

Schwiderski E. W. and Szeto, L. T., 1981, The NSWC global ocean tide data tape (GOTD), its features and application, random-point tide program, *NSWC-TR 81-254,* Naval Surface Weapons Center, Dahlgren Va., 19 pp.

Tamura Y., 1987: A harmonic development of the tide-generating potential, *Bull. d'Inform. Marées Terr.*, **99**, 6813–6855.

Watkins M.M. and Eanes R.J., 1997: Observations of tidally coherent diurnal and semidiurnal variations in the geocenter, *Geophys. Res. Letters,* **24**, 2231–2234.

Webb F H, Zumberge J F, 1993: An Introduction to GIPSY/OASIS-II Precision Software for the Analysis

of Data from the Global Positioning System, *JPL Publ. No. D-11088*, Jet Propulsion Laboratory, Pasadena, Cal.

Zumberge J F, Heflin M B, Jefferson D C, Watkins M M, Webb F H, 1997: Precise point positioning for the efficient and robust analysis of GPS data from large networks. *J. Geophys. Res.*, **102**, 5005–5017

APPENDIX

File names

Air pressure driven geocentre motion: `ftp://gere.oso.chalmers.se/pub/hgs/geoc/airp_$MOD.cmc` where `$MOD` is `ib` (inverted barometer), `noib` (no inverted barometer) or `ocib` (inverted barometer with inforced ocean mass conservation). Explanations in `ftp://gere.oso.chalmers.se/pub/hgs/-INDEX.html`.

Geocentre tide coefficients equivalent to table 1: `ftp://gere.oso.chalmers.se/pub/hgs/geoc/$N.cmc` where `$N` is `S`, `L`, `C` or `CW` is in the text above.

A sideshow with tide analysis results and colour images of the kind of figures in this report can be visited at `ftp://gere.oso.chalmers.se/pub/hgs/4fhw/`.